Chemical Engineering Journal 405 (2021) 126988

Contents lists available at ScienceDirect

Chemical Engineering Journal

journal homepage: www.elsevier.com/locate/cej

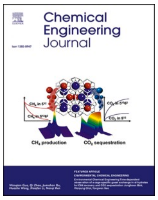

Carbon dots for epoxy curing: Anti-forgery patterns with long-term luminescent stability

Unhan Lee[a], Eunseo Heo[a], Thanh-Hai Le[a], Haney Lee[b], Semin Kim[a], Sanghyuck Lee[a], Hyemi Jo[a], Hyeonseok Yoon[a,b,*]

[a] *Department of Polymer Engineering, Graduate School, Chonnam National University, 77 Yongbong-ro, Buk-gu, Gwangju 61186, South Korea*
[b] *Alan G. MacDiarmid Energy Research Institute & School of Polymer Science and Engineering, Chonnam National University, 77 Yongbong-ro, Buk-gu, Gwangju 61186, South Korea*

ARTICLE INFO

Keywords:
Carbon dots
Epoxy
Curing
Photoluminescence
Nanocomposites

ABSTRACT

Here, we demonstrate that pristine CDs, obtained from amine-containing precursors, were available for the curing of epoxy monomers. The optical properties and the surface chemical functionality of the CDs depended on the nature of the precursors. The CDs showed good compatibility with the epoxy monomer before and during the curing reaction, which led to their uniform dispersion in the epoxy matrix. In addition, it was found that the direct growth of the epoxy chains on the CD surface led to the effective passivation of the CDs. The CD/epoxy nanocomposites showed retentions of more than 80% in PL intensity even after 8 weeks of storage in ambient conditions. Together with those beneficial properties, the CD/precursors were readily patterned or printed on various substrates. The chemical components of the luminescent CDs are similar with the epoxy matrix and furthermore are common in various organic substrates, prohibiting reverse engineering. The combination of the CD/epoxy resin showed strong potential for stealth patterning and printing to enhance anti-forgery protection. Importantly, the use of CDs as curing agents can be further extended to other various kinds of resins.

1. Introduction

Epoxy resins, some of the most important engineering polymers, are extensively used for various practical applications such as painting, coating [1–3], encapsulating [4–6], and packaging [7,8], owing to their excellent mechanical and thermal-/electrical-insulating properties and chemical stability [9–13]. The major characteristics of epoxy resins depend on the curing conditions, including the type of monomer, type and concentration of curing agent and catalyst, and temperature. Several different types of curing agents based on amines, amides, and acid anhydrides have been developed; among these, amine-based agents are the most popular. Typically, the epoxide rings of epoxy monomers with a functionality greater than two react with hydrogen atoms on the curing agent to yield a cross-linked epoxy resin. Bisphenol A diglycidyl ether, a typical epoxy monomer that is commonly derived from the reaction of 2,2-bis(4-hydroxyphenyl)propane (bisphenol A) and 1-chloro-2,3-epoxypropane (epichlorohydrin), has been used with curing agents such as polyamines, polyaminoamides, and acid anhydrides. Many different bisphenol-based epoxy monomers, which are diphenylmethane derivatives, have been synthesized and successfully exploited with other materials for a wide range of end-user applications. Depending on the requirements for specific applications, various combinations of epoxy resins, curing agents, and fillers can be formulated to yield the desired physical/chemical properties [14].

Carbon dots (CDs) belong to a class of carbon-based sub-ten-nanometer nanoparticles. As suggested by the name, CDs have emerged as potential candidates to replace traditional inorganic semiconductor quantum dots as they have exhibited similar if not even identical optical properties [15–18]. A variety of precursors have been used to produce CDs, such as small molecules and natural/synthetic polymers [19–22]. Although the origin of the luminescence of CDs remains unclear, some can emit strong photoluminescence (PL), which has led to their use in imaging, lighting, and sensing [23–28]. It has been found that the optical properties of CDs are significantly affected by their surface passivation or functionalization [29–32]. Heteroatoms can also be incorporated into CDs to tune their optical properties. However, the PL properties of CDs tend to rapidly degrade in air, which has been the greatest obstacle to their widespread use in practical applications. A few

---

* Corresponding author at: School of Polymer Science and Engineering, Chonnam National University, 77 Yongbong-ro, Buk-gu, Gwangju 61186, South Korea.
E-mail address: hyoon@chonnam.ac.kr (H. Yoon).

https://doi.org/10.1016/j.cej.2020.126988
Received 7 July 2020; Received in revised form 25 August 2020; Accepted 7 September 2020

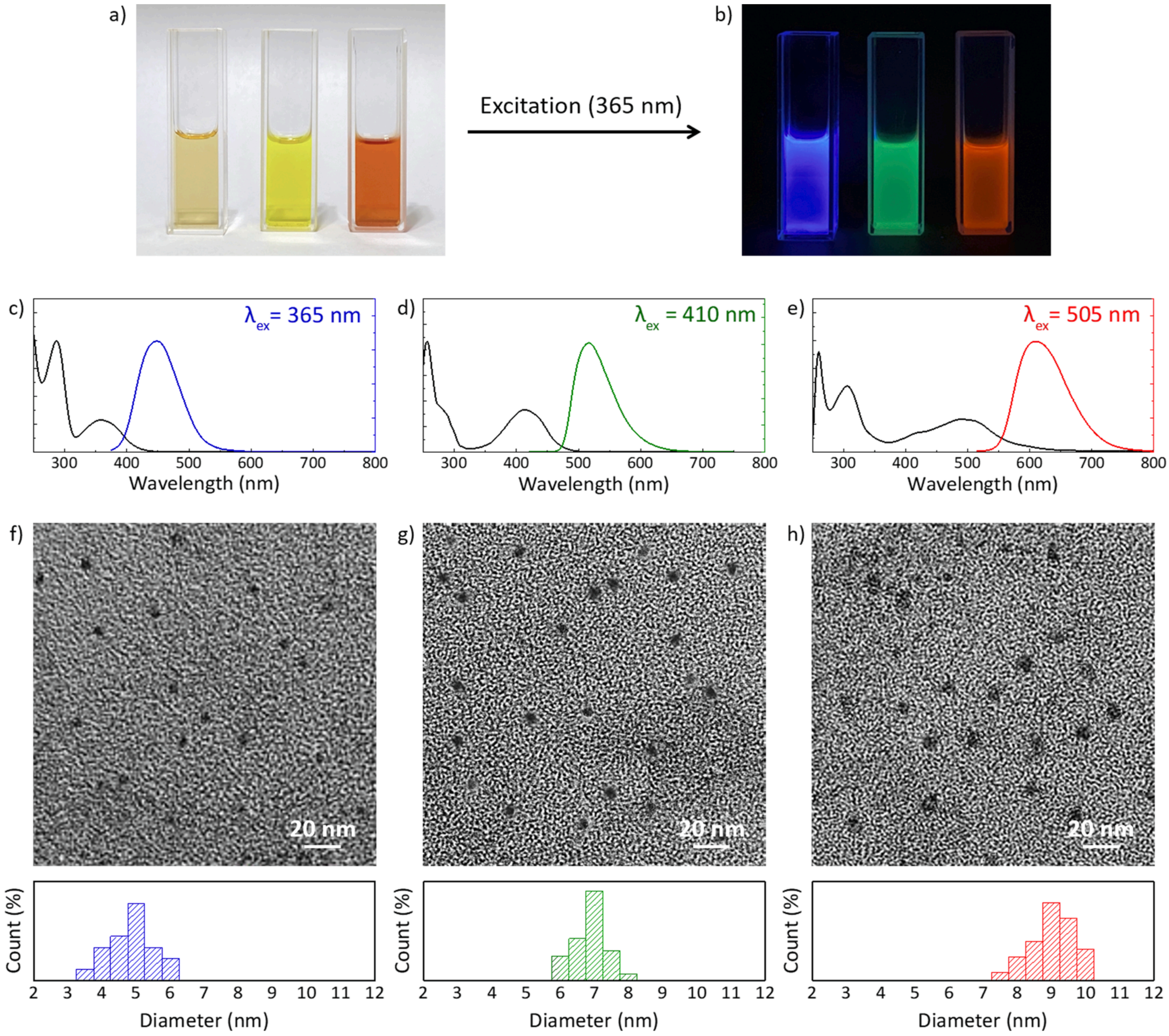

Fig. 1. Photographs of the CDs (left to right: BCDs, GCDs, and RCDs) dispersed in ethanol under (a) room light and (b) 365-nm UV irradiation. UV–visible absorption (black lines) and PL emission (colored lines) spectra of (c) BCDs, (d) GCDs, and (e) RCDs. TEM images of the CDs with histograms showing their particle size distributions: (f) BCDs, (g) GCDs, and (h) RCDs.

examples of incorporating CDs into epoxy matrices have been reported to obtain luminescent composites, in which curing agents and additional surface/interface modification steps were required [33–37].

In this work, we report the first instance of curing epoxy monomers by CDs alone, without any other curing agents, to easily produce luminescent epoxy resins. Three primary-color CDs were prepared using three different amine-containing small molecules as precursors via a bottom-up approach. Importantly, the amine groups originating from the precursor remain on the surface of the CDs to serve as active sites for curing of the epoxy monomers. The use of CDs as the curing agent allowed for the uniform dispersion of the luminescent, few-nanometer-diameter CDs in the epoxy matrix. In addition, the low curing temperature of less than 100 °C enables easy printing/patterning of the CD/epoxy resin on common substrates, such as papers and textiles, without thermal degradation. Furthermore, as the chemical components of the CDs are similar to those of the polymeric substrates, we demonstrated that epoxy curing by CDs can be used for stealth patterning and printing for enhanced anti-forgery applications.

2. Experimental

2.1. Materials

m-Phenylenediamine (*m*-PDA) (99%), *o*-PDA (99%), and *p*-PDA (99%) were purchased from Sigma-Aldrich. A low-viscosity bisphenol A/F-type epoxy monomer, KD-1818, was obtained from Kukdo Chemical, South Korea. *N*,*N*-Dimethylbenzylamine (DMBA, 99%) and ethanol (95%) were purchased from Sigma-Aldrich. Methanol (99.8%) and methylene dichloride (99%) were obtained from Duksan, South Korea.

2.2. Synthesis of CDs

The CDs of different colors, namely blue (BCDs), green (GCDs), and red (RCDs), were synthesized through a solvothermal approach using *m*-PDA, *o*-PDA, and *p*-PDA, respectively [38]. First, 0.5 g (4.624 mmol) of each PDA precursor was dissolved in 50 mL of ethanol. The PDA/ethanol solution was placed in a 100-mL-volume autoclave, which was then heated to 180 °C and maintained for 12 h. After completion of the solvothermal reaction, the resulting product was purified via silica gel

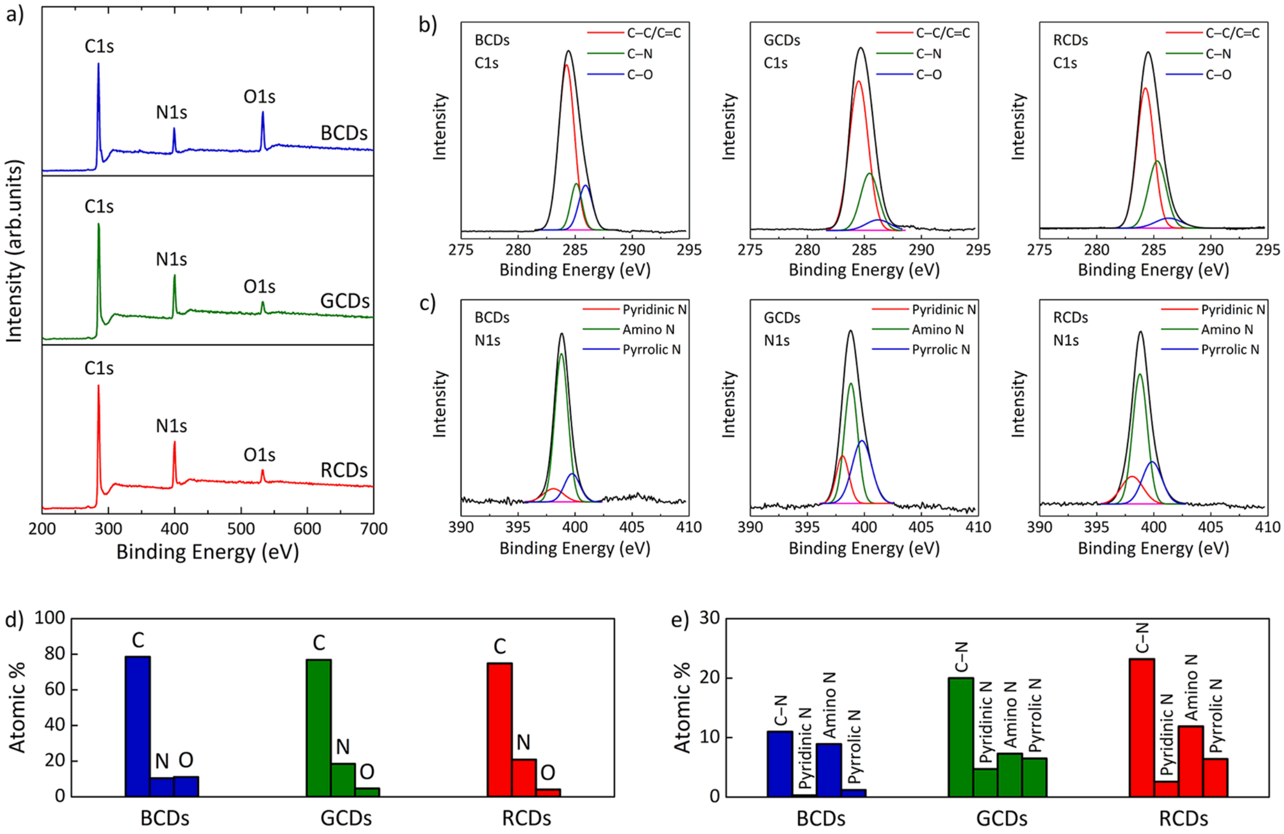

Fig. 2. (a) XP survey spectra and (b, c) high-resolution (b) C 1s and (c) N 1s spectra of the CDs. Deconvoluted components are presented in the high-resolution spectra. (d) Relative contents of C, N, and O elements for BCDs, GCDs, and RCDs determined via XPS. (e) Quantitative fitting results of the XP C 1s (C—N) and N 1s spectra for the BCDs, GCDs, and RCDs.

column chromatography.

2.3. Preparation of CD/epoxy resins

CDs (0.13 g of BCDs, 0.10 g of GCDs, and 0.09 g of RCDs) as the curing agent and DMBA (5 w/w% DMBA/CDs) as the catalyst were dissolved in ethanol and mixed with the epoxy monomer (1.5 g). The mixture was homogenized at 70 °C, poured into a silicone mold (20 mm in diameter and 5 mm in thickness), and held in a vacuum oven at 70 °C for 1 h to allow the bubbles to escape. Subsequently, the temperature of the oven was raised to 90 °C, maintained for 1 h, and finally cooled to room temperature. To obtain thin patterns on the substrates, the homogenized CD/epoxy monomer mixture was placed in a vacuum oven at 90 °C for 10 min. Thereafter, the mixture was screen-printed into a pattern on a substrate and then heated again in a vacuum oven at 90 °C for 1 h.

2.4. Characterization

A Mecasys Optizen 2120UV spectrophotometer was used to record UV–visible absorption spectra of the CDs, and the PL spectra were acquired using a Hitachi F-4500 fluorescence spectrophotometer. Fourier transform infrared (FT-IR) spectra were obtained using a Shimadzu IRAffinity-1S spectrophotometer. X-ray photoelectron spectroscopy (XPS) was performed using a Thermo VG Scientific Multilab 2000 spectrometer, and transmission electron microscopy (TEM) images were acquired using a FEI Tecnai G2 F20 electron microscope. The contact angles were measured using a SurfaceTech GSA-X goniometer.

3. Results and discussion

CDs of different colors, typically blue, green, and red, were synthesized from different precursors via a bottom-up approach, and their surface functionality was further controlled to initiate the curing of epoxy monomers. Three different PDA isomers—*m*-PDA, *o*-PDA, and *p*-PDA—were used to obtain BCDs, GCDs, and RCDs, respectively, via a solvothermal method. The minor differences in the isomer structures have a significant effect on the bottom-up transformation of the precursor molecules into CDs at a high temperature and a high vapor pressure. As shown in Fig. 1a, the obtained CDs exhibited excellent colloidal stability in ethanol, forming clear solutions. The colors of the CD solutions were different even under room light, indicating that they possessed different optical bandgaps. Upon a UV irradiation of 365 nm, as shown in Fig. 1b, the CDs exhibited the desired blue, green, and red emissions. Fig. 1c–e present the UV–visible absorption and PL emission spectra of the CDs. The BCDs, GCDs, and RCDs had absorption bands centered at 365, 410, and 505 nm and maximum PL emission when excited at 445, 515, and 610 nm, respectively. The PL quantum yields (QYs) of the BCDs, GCDs, and RCDs in ethanol were measured as 10.3%, 14.4%, and 20.4%, respectively, under an excitation of 365 nm. Furthermore, the PL QYs of the GCDs and RCDs increased to 20.5% under 410-nm excitation and 26.5% under 505-nm excitation, respectively (Table S1). Fig. 1f–h display the TEM images of the BCDs, GCDs, and RCDs. All the CDs had relatively narrow particle size distributions without any notable aggregation (see the histograms), with diameters of 5.1 ± 1.1, 7.1 ± 0.9, and 9.3 ± 1.3 nm for the BCDs, GCDs, and RCDs, respectively. The emission wavelengths increased with the diameter of the CDs, which is consistent with the trend of inorganic semiconductor quantum dots [39]. In addition to the PL characteristics, it should be noted that the CDs were highly soluble in ethanol. If the CDs were

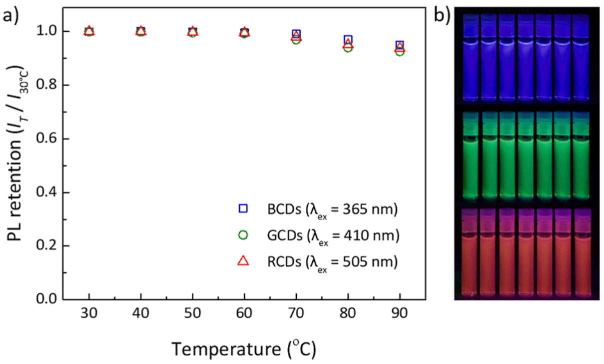

Fig. 3. Variation in PL intensity of the CDs at 30–90 °C. (a) PL intensity was measured as a function of ambient temperature and plotted by dividing it with the initial PL intensity (at 30 °C), and (b) photographs showing the PL retention of the CDs in the temperature range (left to right, taken at an interval of 10 °C under 365 nm excitation).

composed of pure carbon atoms without any surface heteroatoms or functional groups, they would not be soluble in polar solvents. However, the CDs inherit the nitrogen atoms from the amine groups of the precursors, which likely contributes to their excellent colloidal stability in a polar solvent.

The surface functionality of the CDs was examined using XPS. As exhibited in Fig. 2a–c, the XP overview spectra indicated that the CDs consisted of carbon, nitrogen, and oxygen atoms, confirming that they were generated from the precursor PDA without any contamination. The oxygen and nitrogen contents in the CDs were calculated as 4–12% and 10–20%, respectively (Fig. 2d). Clearly, these polar atoms led to an excellent colloidal stability in polar solvents such as ethanol. In addition, the heteroatoms endow the CDs with chemical reactivity, and their contents were found to be different in each CD sample. To gain further in-depth insight into these surface functionalities, the high-resolution XP C 1s and N 1s spectra were deconvoluted into sub-components. First, the C 1s spectrum of the CDs consisted of three peaks corresponding to four functional groups, C—C/C═C, C—N, and C—O, at binding energies of approximately 284.3, 285.2, and 286.1 eV, respectively. The functional groups based on heteroatoms originate from the precursor PDA (atomic ratio of N to C = 1:3) and the ethanol solvent (atomic ratio of O to C = 1:2). The calculated amounts of C—N and C—O components relative to the total amount of carbon were 10.9–23.2% and 3.9–12.8%, which agree with those of the nitrogen and oxygen atoms, respectively, obtained from the overview spectra. The N 1s spectrum of the CDs was deconvoluted into three components at binding energies of 398.1, 398.8, and 399.8 eV corresponding to pyridinic, amino, and pyrrolic nitrogen, respectively. The amounts of different N 1s components for each CD sample are presented in Fig. 2e. While pyridinic nitrogen has no terminal hydrogen atoms, amino nitrogen and pyrrolic nitrogen contain two and one hydrogen atoms, respectively. Considering both the C 1s (C—N component) and N 1s spectra, the amino nitrogen contents were determined as 8.8%, 7.2%, and 12.0% for the BCDs, GCDs, and RCDs, respectively, whereas the respective pyrrolic nitrogen contents were 1.2%, 6.5%, and 6.4%. It is important to note that the hydrogen atoms on pyrrolic and amino nitrogen are active in the curing of the epoxy monomers.

The thermal stability of the CD PL emission is highly important for practical applications. Charge carriers can be trapped by surface states

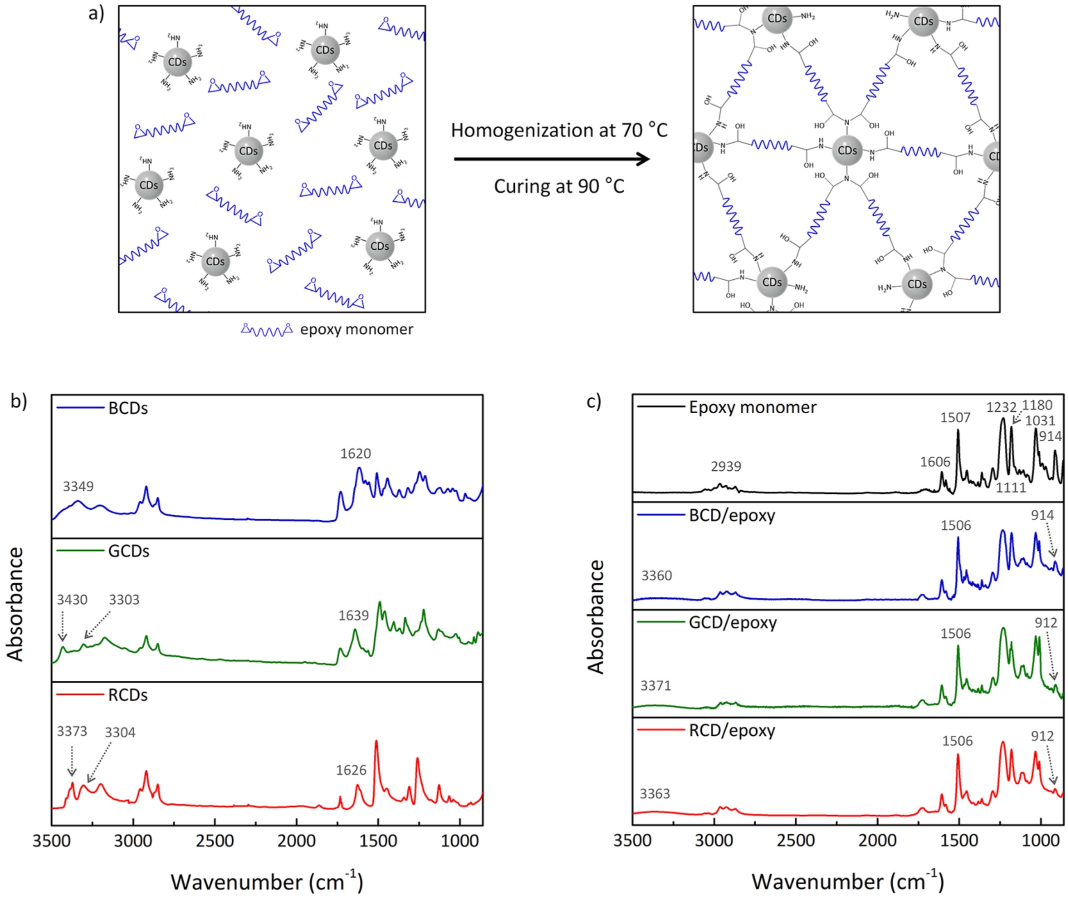

Fig. 4. (a) Scheme representing the curing of epoxy monomers by the CDs. FT-IR spectra of the (b) CDs and (c) resultant CD/epoxy products (the spectrum of the epoxy monomer is provided for a comparison).

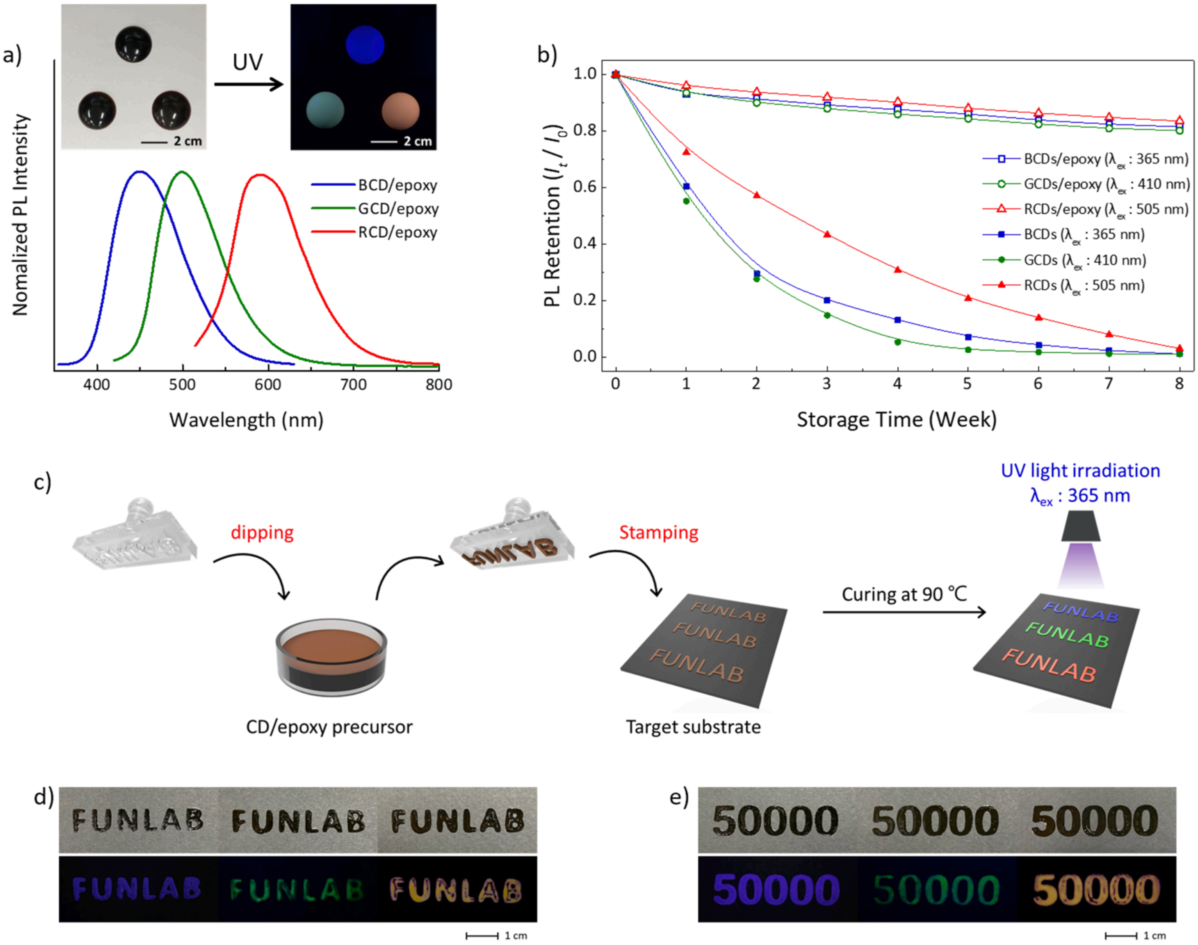

Fig. 5. (a) PL spectra of the CD/epoxy nanocomposites under UV excitation (365 nm) (inset: Photographs of the CD/epoxy nanocomposites before and after UV irradiation). (b) PL retention against storage time: CD/epoxy nanocomposites versus CDs only. (c) Scheme illustrating the CD/epoxy patterning steps on a substrate using a PMMA stamp. Patterns of (d) letters and (e) Arabic numerals stamped on paper under a (above) room light and (bottom) UV lamp (365 nm).

or defects that are thermally activated at elevated temperatures, leading to quenching of the luminescence from CDs [40–43]. Epoxy curing can be performed at high temperatures to facilitate reaction kinetics. However, in several applications, it is desirable for curing to be performed below 100 °C. Therefore, as displayed in Fig. 3, the PL retention of the CDs in the temperature range of 30–90 °C was measured to examine the PL thermal stability. As the ambient temperature increased from 30 to 50 °C, the PL intensity of the CDs remained nearly constant. Upon further increasing the temperature from 60 to 90 °C, the CDs showed only a 5–7% decrease in PL intensity. In general, the luminescent characteristics of CDs depend on the nature of the precursors. For example, CDs prepared hydrothermally from glucose in the presence of glutathione exhibited a ~45% decrease in PL intensity with increasing temperature from 30 to 90 °C [44]. Thus, it is notable that the PL emission of the BCDs, GCDs, and RCDs was well preserved at temperatures near 100 °C.

The most commonly used epoxy resin monomers are diglycidyl ethers based on bisphenol A and bisphenol F. A low-viscosity bisphenol A/F-type liquid epoxy resin, which allows for solvent-free, low-temperature curing conditions, was thus selected as a model epoxy monomer to evaluate the capability of the CDs as functional curing agents. The CDs were mixed with the epoxy monomer at 70 °C for homogenization, and the CD-incorporated monomer was cured at 90 °C. As illustrated in Fig. 4a, functional groups such as amino nitrogen and pyrrolic nitrogen atoms are available for monomer curing on the CD surfaces. FT-IR spectroscopy was employed to determine if the epoxy monomer could be cured using only the CDs without any other curing agents. First, the functionalities of the CDs were characterized, as displayed in Fig. 4b. The three CDs all presented absorption bands related to —OH, C═O, C—C, phenolic hydroxyl, and aromatic ether stretching vibrations at 3175–3204, 1730–1731, 1491–1511, 1309–1366, and 1221–1259 cm^{-1}, respectively. Notably, absorption bands appeared at 3303–3373 and 1620–1639 cm^{-1} corresponding to the primary and secondary amine stretching vibrations, respectively, which are consistent with the XPS analysis. These amino functional groups on the CDs can progress the curing of the epoxy monomer. Fig. 4c presents the FT-IR spectra of the used epoxy monomer and resultant CD/epoxy products (see also the FT-IR spectra of the uncured mixtures in Fig. S3). The epoxy monomer revealed characteristic peaks at 2918–2939, 1606/1507, and 1232–1031 cm^{-1}, which are attributable to C—H stretching, C═C/C—C stretching in aromatic rings, and C—O—C symmetric/asymmetric stretching of aromatic ether and ester groups, respectively. The peak at approximately 914 cm^{-1} is mainly attributable to the oxirane ring. After curing, the intensity of the oxirane ring peak decreased, indicating that the ring participated in the curing reaction, and a broad band arising from secondary amine (N—H) and —OH stretching vibrations appeared at 3360–3371 cm^{-1}. The decreased oxirane ring peak and appearance of —OH and N—H features imply that the curing reaction between the CDs and epoxy monomers occurred successfully (see the calculated curing degrees in Supplementary Information) [33,45].

The uniform dispersion of nanoparticles in polymeric resins remains a challenging task that has hindered the practical application of nanoparticle-incorporated polymer composites. It is important to note that the curing of epoxy monomers by the CDs resulted in CD/epoxy nanocomposites without any sophisticated surface treatment or homogenization processes. The CDs were readily mixed with the liquid-phase epoxy monomer, and no sedimentation during curing or aggregation during post-curing was observed. Fig. 5a displays photos of the as-obtained CD/epoxy nanocomposites, which were translucent despite the colors of the CDs (see also Fig. S5). This means that the CDs have good molecular-level compatibility with the epoxy monomer before and during the curing reaction. Upon UV (365 nm) irradiation, the CD/epoxy nanocomposites yielded blue, green, and red emissions, which were consistent with the emission colors of the CDs used as the curing agents. The PL spectra of the CD/epoxy nanocomposites were also similar to those of the corresponding CDs, except that the emission peaks were slightly blue shifted (Fig. 5a). The PL QYs of the BCD/epoxy, GCD/epoxy, and RCD/epoxy nanocomposites were measured as 5.3%, 8.6%, and 10.2%, respectively, under an excitation of 365 nm. Furthermore, the PL QYs of the GCD/epoxy and RCD/epoxy nanocomposites were 11.4% and 14.1% under 410- and 505-nm excitations, respectively (Table S2). Long-term PL stability of the CD/epoxy nanocomposites is also crucial for their practical utilization. Thus, the emission intensity of the CD/epoxy nanocomposites was monitored under ambient conditions, and the results are shown in Fig. 5b. Notably, the PL intensities of the CD/epoxy nanocomposites decreased by only 16–20% after 8 weeks of storage in air at room temperature. In contrast, the CDs alone completely lost their emission capability after the same storage period. Therefore, it is believed that the direct growth of epoxy chains on their surfaces passivated the CDs. By exploiting their superior properties, the liquid-phase CD/epoxy precursors were readily printed or patterned on various substrates (e.g., papers, textiles, plastics, and glass) and cured at temperatures below 100 °C (Table S3). The low temperature curing enables easy printing/patterning of the CD/epoxy resin on the substrates without thermal degradation and provides moderate mechanical properties suitable for the flexible substrate. More importantly, contrary to inorganic semiconductor quantum dots, the constituent elements of the CDs (carbon, nitrogen, and oxygen) are common to those of other substrates, including the epoxy matrix and the materials mentioned above, making reverse engineering impossible. Therefore, curing epoxy resins using CDs can be employed for stealth patterning and printing to achieve enhanced anti-forgery protection (Fig. 5c). Fig. 5d and e demonstrate that the CD/epoxy precursors can be simply stamped on paper and mildly heat-treated to yield PL patterns of the nanocomposites.

4. Conclusions

Pristine CDs obtained from amine-containing precursors were shown to be applicable for the curing of epoxy monomers. The CDs exhibited good compatibility with the epoxy monomer before and during the curing reaction, which led to their uniform dispersion in the epoxy matrix. In addition, the direct growth of epoxy chains on the CD surfaces led to their effective passivation. The CD/epoxy nanocomposites showed PL intensity retentions of more than 80% after 8 weeks of storage in ambient conditions. The chemical components of the luminescent CDs are similar to those of the epoxy matrix, as well as the components of various organic substrates, thereby prohibiting reverse engineering. Thus, the combination of the CD/epoxy resin shows significant potential for anti-forgery applications. Furthermore, it is important to note that the use of such CDs as curing agents can be extended to other types of resins.

Declaration of Competing Interest

The authors declare that they have no known competing financial interests or personal relationships that could have appeared to influence the work reported in this paper.

Acknowledgments

This research was supported by Basic Science Research Program through the National Research Foundation of Korea (NRF), funded by the Ministry of Education (NRF- 2020R1I1A3072666).

Appendix A. Supplementary data

Supplementary data to this article can be found online at https://doi.org/10.1016/j.cej.2020.126988.

References

[1] M. Cui, S. Ren, H. Zhao, Q. Xue, L. Wang, Polydopamine coated graphene oxide for anticorrosive reinforcement of water-borne epoxy coating, Chem. Eng. J. 335 (2018) 255–266.

[2] X. Zhang, Z. Liu, Y. Li, C. Wang, Y. Zhu, H. Wang, J. Wang, Robust superhydrophobic epoxy composite coating prepared by dual interfacial enhancement, Chem. Eng. J. 371 (2019) 276–285.

[3] H. Zhou, R. Chen, Q. Liu, J. Liu, J. Yu, C. Wang, M. Zhang, P. Liu, J. Wang, Fabrication of ZnO/epoxy resin superhydrophobic coating on AZ31 magnesium alloy, Chem. Eng. J. 368 (2019) 261–272.

[4] X. Wang, P. Wu, Melamine foam-supported 3D interconnected boron nitride nanosheets network encapsulated in epoxy to achieve significant thermal conductivity enhancement at an ultralow filler loading, Chem. Eng. J. 348 (2018) 723–731.

[5] S. Jia, X. Lu, S. Luo, Y. Qing, N. Yan, Y. Wu, Efficiently texturing hierarchical epoxy layer for smart superhydrophobic surfaces with excellent durability and exceptional stability exposed to fire, Chem. Eng. J. 348 (2018) 212–223.

[6] K.-H. Jung, K.D. Min, C.-J. Lee, B.-G. Park, H. Jeong, J.-M. Koo, B. Lee, S.-B. Jung, Effect of epoxy content in Ag nanoparticle paste on the bonding strength of MLCC packages, Appl. Surf. Sci. 495 (2019), 143487.

[7] C. Chen, Y. Xue, X. Li, Y. Wen, J. Liu, Z. Xue, D. Shi, X. Zhou, X. Xie, Y.-W. Mai, High-performance epoxy/binary spherical alumina composite as underfill material for electronic packaging, Compos. Part A Appl. Sci. Manuf. 118 (2019) 67–74.

[8] D. Lee, S. Lee, S. Byun, K.-W. Paik, S.H. Song, Novel dielectric BN/epoxy nanocomposites with enhanced heat dissipation performance for electronic packaging, Compos. Part A Appl. Sci. Manuf. 107 (2018) 217–223.

[9] H. Liu, H. Zhang, H. Wang, X. Huang, G. Huang, J. Wu, Weldable, malleable and programmable epoxy vitrimers with high mechanical properties and water insensitivity, Chem. Eng. J. 368 (2019) 61–70.

[10] H. Duan, Y. Chen, S. Ji, R. Hu, H. Ma, A novel phosphorus/nitrogen-containing polycarboxylic acid endowing epoxy resin with excellent flame retardance and mechanical properties, Chem. Eng. J. 375 (2019), 121916.

[11] X. Fan, G. Zhang, Q. Gao, J. Li, Z. Shang, H. Zhang, Y. Zhang, X. Shi, J. Qin, Highly expansive, thermally insulating epoxy/Ag nanosheet composite foam for electromagnetic interference shielding, Chem. Eng. J. 372 (2019) 191–202.

[12] Y.-J. Xu, L. Chen, W.-H. Rao, M. Qi, D.-M. Guo, W. Liao, Y.-Z. Wang, Latent curing epoxy system with excellent thermal stability, flame retardance and dielectric property, Chem. Eng. J. 347 (2018) 223–232.

[13] M. Owais, J. Zhao, A. Imani, G. Wang, H. Zhang, Z. Zhang, Synergetic effect of hybrid fillers of boron nitride, graphene nanoplatelets, and short carbon fibers for enhanced thermal conductivity and electrical resistivity of epoxy nanocomposites, Compos. Part A Appl. Sci. Manuf. 117 (2019) 11–22.

[14] L. Guadagno, C. Naddeo, M. Raimondo, G. Barra, L. Vertuccio, S. Russo, K. Lafdi, V. Tucci, G. Spinelli, P. Lamberti, Influence of carbon nanoparticles/epoxy matrix interaction on mechanical, electrical and transport properties of structural advanced materials, Nanotechnology 28 (2017), 094001.

[15] Y. Choi, Y. Choi, O.-H. Kwon, B.-S. Kim, Carbon dots: bottom-up syntheses, properties, and light-harvesting applications, Chem. Asian J. 13 (2018) 586–598.

[16] T.-H. Le, Y. Choi, H. Han, S. Noh, C.S. Park, S. Kim, S. Chae, H.J. Kim, W.B. Im, T. H. Ha, O.S. Kwon, H. Yoon, Highly luminescent quantum dots in remote-type liquid-phase color converters for white light-emitting diodes, Adv. Mater. Technol. 3 (2018) 1800235.

[17] T.-H. Le, Y. Choi, S. Kim, U. Lee, E. Heo, H. Lee, S. Chae, W.B. Im, H. Yoon, Highly elastic and >200% reversibly stretchable down-conversion white light-emitting diodes based on quantum dot gel emitters, Adv. Opt. Mater. 8 (2020) 1901972.

[18] J. Jung, M. Chang, H. Yoon, Interface engineering strategies for fabricating nanocrystal-based organic-inorganic nanocomposites, Appl. Sci. 8 (2018) 1376.

[19] T.-H. Le, H. Yoon, Strategies for fabricating versatile carbon nanomaterials from polymer precursors, Carbon 152 (2019) 796–817.

[20] W. Wang, Z. Zeng, G. Zeng, C. Zhang, R. Xiao, C. Zhou, W. Xiong, Y. Yang, L. Lei, Y. Liu, D. Huang, M. Cheng, Y. Yang, Y. Fu, H. Luo, Y. Zhou, Sulfur doped carbon quantum dots loaded hollow tubular g-C3N4 as novel photocatalyst for destruction of Escherichia coli and tetracycline degradation under visible light, Chem. Eng. J. 378 (2019), 122132.

[21] H. Liu, L. Ding, L. Chen, Y. Chen, T. Zhou, H. Li, Y. Xu, L. Zhao, N. Huang, A facile, green synthesis of biomass carbon dots coupled with molecularly imprinted polymers for highly selective detection of oxytetracycline, J. Ind. Eng. Chem. 69 (2019) 455–463.

[22] N.A. Travlou, J. Secor, T.J. Bandosz, Highly luminescent S-doped carbon dots for the selective detection of ammonia, Carbon 114 (2017) 544–556.

[23] S.Y. Lim, W. Shen, Z. Gao, Carbon quantum dots and their applications, Chem. Soc. Rev. 44 (2015) 362–381.

[24] V. Strauss, J.T. Margraf, C. Dolle, B. Butz, T.J. Nacken, J. Walter, W. Bauer, W. Peukert, E. Spiecker, T. Clark, D.M. Guldi, Carbon nanodots: toward a comprehensive understanding of their photoluminescence, J. Am. Chem. Soc. 136 (2014) 17308–17316.

[25] P. Gong, L. Sun, F. Wang, X. Liu, Z. Yan, M. Wang, L. Zhang, Z. Tian, Z. Liu, J. You, Highly fluorescent N-doped carbon dots with two-photon emission for ultrasensitive detection of tumor marker and visual monitor anticancer drug loading and delivery, Chem. Eng. J. 356 (2019) 994–1002.

[26] S.M. Ardekani, A. Dehghani, M. Hassan, M. Kianinia, I. Aharonovich, V.G. Gomes, Two-photon excitation triggers combined chemo-photothermal therapy via doped carbon nanohybrid dots for effective breast cancer treatment, Chem. Eng. J. 330 (2017) 651–662.

[27] S. Zhao, S. Wu, Q. Jia, L. Huang, M. Lan, P. Wang, W. Zhang, Lysosome-targetable carbon dots for highly efficient photothermal/photodynamic synergistic cancer therapy and photoacoustic/two-photon excited fluorescence imaging, Chem. Eng. J. 388 (2020), 124212.

[28] L. Zheng, P. Qi, D. Zhang, Identification of bacteria by a fluorescence sensor array based on three kinds of receptors functionalized carbon dots, Sens. Actuat. B Chem. 286 (2019) 206–213.

[29] A. Kundu, J. Lee, B. Park, C. Ray, K.V. Sankar, W.S. Kim, S.H. Lee, I.-J. Cho, S. C. Jun, Facile approach to synthesize highly fluorescent multicolor emissive carbon dots via surface functionalization for cellular imaging, J. Colloid Interface Sci. 513 (2018) 505–514.

[30] S. Sidhik, J. Velusamy, E. De la Rosa, S.A. Pérez-García, G. Ramos-Ortiz, T. López-Luke, Role of carbon nanodots in defect passivation and photo-sensitization of mesoscopic-TiO_2 for perovskite solar cells, Carbon 146 (2019) 388–398.

[31] K. Gao, Y. Guo, Q. Niu, L. Han, L. Zhou, L. Wang, Quaternary ammonium-functionalized carbon dots for sensitive and selective detection of 2,4,6-trinitrophenol in aqueous medium, Sens. Actuat. B Chem. 262 (2018) 298–305.

[32] X. Hou, Y. Hu, P. Wang, L. Yang, M.M. Al Awak, Y. Tang, F.K. Twara, H. Qian, Y.-P. Sun, Modified facile synthesis for quantitatively fluorescent carbon dots, Carbon 122 (2017) 389-394.

[33] B. De, B. Voit, N. Karak, Transparent luminescent hyperbranched epoxy/carbon oxide dot nanocomposites with outstanding toughness and ductility, ACS Appl. Mater. Interf. 5 (2013) 10027–10034.

[34] L. Chen, C. Zhang, Z. Du, H. Li, L. Zhang, W. Zou, Fabrication of carboxyl group-functionalized carbon quantum dots and its transparent and luminescent epoxy matrix nanocomposites for white LED encapsulation, Macromol. Mater. Eng. 300 (2015) 1232–1237.

[35] Z. Zhou, P. Tian, X. Liu, S. Mei, D. Zhou, D. Li, P. Jing, W. Zhang, R. Guo, S. Qu, A. L. Rogach, Hydrogen peroxide-treated carbon dot phosphor with a bathochromic-shifted, aggregation-enhanced emission for light-emitting devices and visible light communication, Adv. Sci. 5 (2018) 1800369.

[36] M. George, A. Mohanty, Investigation of mechanical properties of graphene decorated with graphene quantum dot-reinforced epoxy nanocomposite, J. Appl. Polym. Sci 137 (2020) 48680.

[37] H. Zhang, J. You, J. Wang, X. Dong, R. Guan, D. Cao, Highly luminescent carbon dots as temperature sensors and “off-on” sensing of Hg^{2+} and biothiols, Dyes Pigm. 173 (2020), 107950.

[38] K. Jiang, S. Sun, L. Zhang, Y. Lu, A. Wu, C. Cai, H. Lin, Red, green, and blue luminescence by carbon dots: full-color emission tuning and multicolor cellular imaging, Angew. Chem. Int. Ed. 54 (2015) 5360–5363.

[39] H.-C. Wang, S.-Y. Lin, A.-C. Tang, B.P. Singh, H.-C. Tong, C.-Y. Chen, Y.-C. Lee, T.-L. Tsai, R.-S. Liu, Mesoporous silica particles integrated with all-inorganic CsPbBr 3 perovskite quantum-dot nanocomposites (MP-PQDs) with high stability and wide color gamut used for backlight display, Angew. Chem. Int. Ed. 55 (2016) 7924–7929.

[40] S. Hu, W. Yang, N. Li, H. Wang, J. Yang, Q. Chang, Carbon-dot-based heterojunction for engineering band-edge position and photocatalytic performance, Small 14 (2018) 1803447.

[41] Y. Liu, L. Zhou, Y. Li, R. Deng, H. Zhang, Highly fluorescent nitrogen-doped carbon dots with excellent thermal and photo stability applied as invisible ink for loading important information and anti-counterfeiting, Nanoscale 9 (2017) 491–496.

[42] D. Zhou, Y. Zhai, S. Qu, D. Li, P. Jing, W. Ji, D. Shen, A.L. Rogach, Electrostatic assembly guided synthesis of highly luminescent carbon-nanodots@$BaSO_4$ hybrid phosphors with improved stability, Small 13 (2017) 1602055.

[43] Y. Zhao, C. Riemersma, F. Pietra, R. Koole, C. de Mello Donegá, A. Meijerink, High-temperature luminescence quenching of colloidal quantum dots, ACS Nano 6 (2012) 9058–9067.

[44] C. Wang, Z. Xu, H. Cheng, H. Lin, M.G. Humphrey, C. Zhang, A hydrothermal route to water-stable luminescent carbon dots as nanosensors for pH and temperature, Carbon 82 (2015) 87–95.

[45] M. Garg, S. Sharma, R. Mehta, Pristine and amino functionalized carbon nanotubes reinforced glass fiber epoxy composites, Compos. Part A Appl. Sci. Manuf. 76 (2015) 92–101.